Journal of Power Sources 196 (2011) 6196–6200

Contents lists available at ScienceDirect

Journal of Power Sources

journal homepage: www.elsevier.com/locate/jpowsour

Short communication

Improved high temperature performance of $La_{0.8}Sr_{0.2}MnO_3$ cathode by addition of CeO_2

J.P. Wiff*, K. Jono, M. Suzuki, S. Suda

Japan Fine Ceramics Center (JFCC), 2-4-1 Mutsuno, Atsuta-ku, Nagoya, Aichi-ken 456-8587, Japan

ARTICLE INFO

Article history:
Received 7 January 2011
Received in revised form 4 March 2011
Accepted 29 March 2011
Available online 12 April 2011

Keywords:
SOFC cell
LSM
High temperature
Co-sintering
$La_2Zr_2O_7$
CeO_2

ABSTRACT

Ceria is proposed as an additive for $La_{0.8}Sr_{0.2}MnO_3$ (LSM) cathodes in order to increase both their thermal stability and electrochemical properties after co-sintering with an yttria-stabilized zirconia (YSZ) electrolyte at 1350 °C. Results show that LSM without CeO_2 addition is unstable at 1350 °C, whereas the thermal stability of LSM is drastically improved after addition of CeO_2. In addition, results show a correlation between CeO_2 addition and the maximum power density obtained in 300 μm thick electrolyte-supported single cells in which the anode and modified cathode have been co-sintered at 1350 °C. Single cells with cathodes not containing CeO_2 produce only 7 mW cm^{-2} at 800 °C, whereas the power density increases to 117 mW cm^{-2} for a CeO_2 addition of 12 mol%. Preliminary results suggest that CeO_2 could increase the power density by at least two mechanisms: (1) incorporation of cerium into the LSM crystal structure, and (2) by modification or reduction of $La_2Zr_2O_7$ formation at high temperature. This approach permits the highest LSM–YSZ co-sintering temperature so far reported, providing power densities of hundreds of mW cm^{-2} without the need for a buffer layer between the LSM cathode and YSZ electrolyte. Therefore, this method simplifies the co-sintering of SOFC cells at high temperature and improves their electrochemical performance.

1. Introduction

Strontium-doped lanthanum manganite (LSM) is commonly used in the fabrication of solid oxide fuel cells (SOFCs) as the cathode material, because it displays good electrical conductivity, electrocatalytic activity and high thermal and chemical stability between 800 °C and 1000 °C [1–4]. However, at higher temperatures (>1100 °C) LSM reacts with yttria-stabilized zirconia (YSZ) to form either lanthanum zirconate, $La_2Zr_2O_7$ (LZO), or strontium zirconate, $SrZrO_3$ (SZO), at the contact zone, thereby decreasing both the cathode and single cell electrochemical performance [4–6]. Several approaches, with different technical complexities, have been attempted in order to reduce the reaction between LSM and YSZ at high temperature, for example, introducing a gadolinia-doped-ceria-based interlayer [7], using a cathode composed of a certain mixture of LSM and YSZ [8], or optimizing the Sr content [9]. However, even using these approaches the highest sintering temperature for LSM remains below the minimum sintering temperature for YSZ (~1350 °C). Hence, LSM and YSZ currently cannot be co-sintered at temperatures as high as 1350 °C without obtaining SOFC cells with extremely poor electrochemical performance.

Recently, Konysheva et al. reported the crystal structures and electrical and magnetic properties of phases in the $La_{0.8}Sr_{0.2}MnO_3$–CeO_2 system [10]. They characterized the crystal structures of different phases formed between $La_{0.8}Sr_{0.2}MnO_3$ and CeO_2 at 1350 °C and additionally established the solubility limit of CeO_2 into LSM at about 2 mol% [10]. In addition, they showed that for CeO_2 contents between 2 and 10 mol% a slight increase in electrical conductivity is induced. Their work thus demonstrated that CeO_2 addition can change the electrical properties of LSM. However, up to now there have been no more reports of the effect of CeO_2 addition on the thermal stability or electrochemical performance of LSM cathodes.

In this paper we examine the use of different CeO_2 additions into LSM cathode materials in an attempt to increase the thermal stability of LSM at 1350 °C, modify or reduce the formation of high electrical resistant secondary phases (LZO or SZO) during co-sintering with YSZ, and thereby increase the power density of YSZ-based single cells using LSM as the cathode. After describing the experimental methods used, we present results showing that CeO_2 addition has a beneficial effect on LSM cathode materials, and conclude that it may be a very simple and effective strategy for enabling the use of LSM-cathode and YSZ-electrolyte in SOFC cells produced by co-sintered at 1350 °C.

* Corresponding author. Tel.: +81 52 871 3500; fax: +81 52 871 3599.
E-mail addresses: jpwiff@jpwiff.com, jpwiff@jfcc.or.jp (J.P. Wiff).

0378-7753/$ – see front matter © 2011 Elsevier B.V. All rights reserved.
doi:10.1016/j.jpowsour.2011.03.102

2. Experimental procedures

2.1. Preparation of LSM powders with CeO_2 addition

10 mol% CeO_2-added $La_{0.8}Sr_{0.2}MnO_3$ powders were prepared by mixing commercial powders of $La_{0.8}Sr_{0.2}MnO_3$ (d_{50} = 0.3 μm; AGC Seimi Chemical Co., Japan) and CeO_2 (Mitsuwa Pure Chemical, Japan) in ethanol overnight and then drying them at 60 °C under vacuum.

Several pellets of CeO_2-added $La_{0.8}Sr_{0.2}MnO_3$ (Ce–LSM) were fabricated by cold isostatic pressing (CIP) powders at 2.5 tonnes for 5 min and then sintering at 1350 °C for 5 h in air. Pellets of $La_{0.8}Sr_{0.2}MnO_3$ (LSM) without CeO_2 were also prepared for comparison in order to evaluate their thermal stabilities at high temperature. Another set of pellets was prepared by mixing either LSM or Ce–LSM powders with 50 wt% YSZ (TZ8Y, Tosoh Corporation, Japan), in order to evaluate the thermal stability of LSM during co-sintering with YSZ at high temperature.

X-ray diffraction (XRD) in a $\theta/2\theta$ configuration (Rigaku RINT, CuKα, with a graphite monochromator) was used for identifying crystallographic phases in all samples. The diffractometer was mechanically aligned and the recorded XRD patterns normalized in order to ensure a consistent comparison. X-ray photoelectron spectroscopy (XPS), with monochromatic AlKα source, was used for characterizing the oxidation state in LSM and Ce–LSM samples after sintering at 1350 °C. Signals O1s and C1s were used as reference in order to ensure the curve fit analysis. Scanning electron microscopy (SEM) was used to observe the microstructure after sintering at high temperature.

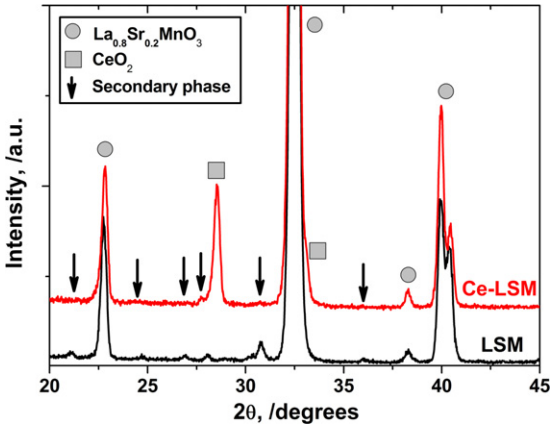

Fig. 1. XRD patterns of LSM and Ce–LSM pellets after sintering at 1350 °C for 5 h.

2.2. Evaluation of cathode and single cell performance after sintering

YSZ-electrolyte-supported single cells were fabricated by screen printing. Both porous anode (Ni–YSZ) and cathode pastes were screen-printed on a 300 μm thick electrolyte and then co-sintered at 1350 °C for 5 h in air using heating and cooling rates of 200 °C h^{-1}. Several Ce–LSM cathode compositions were prepared in the manner described in section 2.1 using different amounts of CeO_2, namely 0, 4, 8, 12 and 15 mol%. Electrochemical evaluation was carried out at 800 °C with H_2 + 3% H_2O and dry air

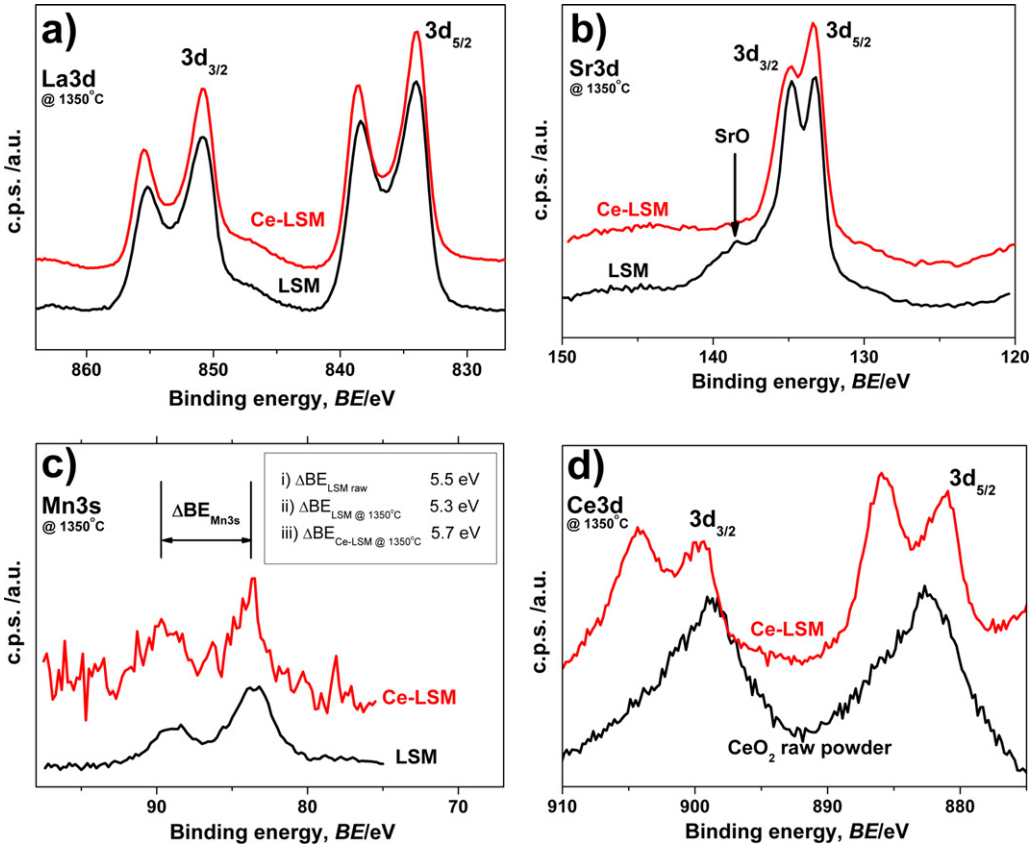

Fig. 2. (a), (b) and (c) XPS spectra of La3d, Sr3d and Mn3s from LSM and Ce–LSM pellets sintered at 1350 °C, respectively. (d) XPS spectra of Ce3d from Ce and Ce–LSM pellets sintered at 1350 °C.

at the anode and cathode sides, respectively, using flow rates of 50 ml min^{-1}.

3. Results and discussion

3.1. Enhancement of $La_{0.8}Sr_{0.2}MnO_3$ cathode stability at high temperature

Fig. 1 shows the XRD patterns of LSM and Ce–LSM pellets sintered at 1350 °C for 5 h in air. Both XRD patterns indicate $La_{0.8}Sr_{0.2}MnO_3$ is the main phase. However, in LSM pellets without CeO_2, the formation of one or more minor phases is also apparent, consistent with the thermal instability of LSM at 1350 °C. In contrast, in Ce–LSM pellets the amount of minor phases was drastically reduced, suggesting that Ce–LSM pellets exhibit enhanced thermal stability with respect to LSM pellets at 1350 °C.

Fig. 2a–c show the XPS spectra of La3d, Sr3d and Mn3s from LSM and Ce–LSM pellets sintered at 1350 °C, respectively. Manganese oxidation state was estimated by using the binding energy gap (ΔBE_{Mn3s}) indicated in Fig. 2c, thus when ΔBE_{Mn3s} = {4.5, 5.5 or 6.5 eV} the manganese oxidation state corresponds to Mn (IV), Mn (III) or Mn (II), respectively [11].

Fig. 2a shows no difference between the La3d signals from LSM and Ce–LSM pellets. Both spectra show a quadruplet instead of the characteristic $La3d_{3/2}$ and $La3_{d5/2}$ duplet caused by the spin–orbit interaction. This quadruplet effect has been reported in similar LSM perovskite cathodes and it is caused by electron transference from the oxygen ligands to the initially unfilled La4f orbital [12].

Fig. 2b shows a significant difference between Sr3d signals from LSM and Ce–LSM sintered pellets: an additional peak at 138 eV, assigned as SrO, is observed only in the LSM pellets, whereas in the Ce–LSM it is completely avoided. This effect is in agreement with Fig. 1 supporting that CeO_2 addition could increases the thermal stability of LSM.

Fig. 2c indicates the binding energy gap (ΔBE_{Mn3s}) used for estimating the oxidation state of manganese. Inset shows the ΔBE_{Mn3s} observed in (i) LSM raw powder and (ii) LSM pellet at 1350 °C and (iii) Ce–LSM pellet at 1350 °C, suggesting that in raw powders the manganese is mainly present as Mn (III), whereas in the LSM pellet the oxidation state tends to slightly increases because the thermal instability observed in Fig. 2b, and contrarily, in the Ce–LSM pellet the oxidation state tends to slightly decrease due to a charge compensation mechanism caused by the CeO_2 addition.

Fig. 2d shows the XPS spectrum of Ce3d from CeO_2 and Ce–LSM pellets sintered at 1350 °C. Ce3d signal from CeO_2 shows the characteristic $Ce3d_{3/2}$ and $Ce3_{d5/2}$ duplet with wide peaks because the electrical charge during the XPS analysis. However, the Ce3d signal from Ce–LSM shows a quadruplet as well as it is observed for La3d (Fig. 2a), suggesting that Ce could react with LSM and probably plays a role in the thermal stability enhancement of LSM cathode at high temperature.

Fig. 3a and b show the microstructure of LSM and Ce–LSM pellets, respectively, after sintering at 1350 °C for 5 h in air. Some differences between the microstructures are noticeable: (i) The grain size is smaller in Ce–LSM pellets than LSM pellets; (ii) LSM pellets show some step- and bubble-like features on the surface, whereas these are not observed on Ce–LSM pellet surfaces; and (iii) the insets show that in LSM pellets some manganese oxide crystals are formed on the surface, whereas in Ce–LSM pellets they are not. The first effect can be explained in terms of the low solubility of CeO_2 in $La_{0.8}Sr_{0.2}MnO_3$ [10], with excess CeO_2 accumulating at LSM grain boundaries, thus restricting the grain growth. The second observation suggests the LSM sample contains partially melted grain boundaries, since these can give rise to both step- and bubble-like structures. The third observation is in agreement with previous work, in which some manganese oxide crystals were formed on the surface of LSM under similar heat treatment conditions [13]. The SEM observations are thus consistent with the conclusion that CeO_2 addition enhances the thermal stability of LSM at 1350 °C.

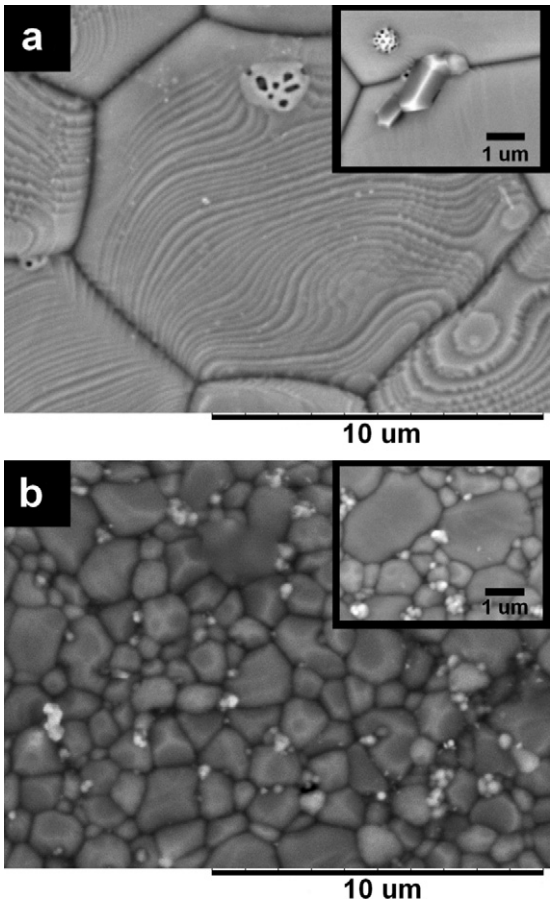

Fig. 3. Microstructures of (a) LSM and (b) Ce–LSM after sintering at 1350 °C for 5 h, respectively. Insets show magnified regions.

The improved thermal stability of Ce–LSM powders makes them attractive for preparing SOFC single cells by co-sintering with an YSZ electrolyte at high temperature. This should affect the formation of LZO or SZO, thereby leading to improvements in the electrochemical performance of the cathode. The stability of Ce–LSM powders co-sintered with YSZ was evaluated firstly by XRD.

Fig. 4 shows the XRD patterns of LSM–YSZ and Ce–LSM–YSZ pellets after sintering at 1350 °C compared with Ce–LSM–YSZ mixed powder at room temperature (RT). Regardless of sample composition or heat treatment temperature, no formation of SZO phase was observed.

The main diffraction peaks of the Ce–LSM–YSZ powder at room temperature correspond to YSZ ($2\theta = 29.98°$) and CeO_2 ($2\theta = 28.54°$) phases. The pattern for LSM–YSZ at 1350 °C shows an additional peak at $2\theta = 28.66°$ in agreement with the formation of LZO (JCPDS #73-0444) [14,15]. The XRD pattern for Ce–LSM–YSZ at 1350 °C reveals at least three fascinating effects. First, no CeO_2 peaks are observed. The CeO_2 must therefore have reacted with YSZ because the XRD pattern in Fig. 1 showed that, for the most part, CeO_2 is thermally stable in contact with LSM at 1350 °C. Second, the LZO peak appears to have slightly shifted to 2θ=28.73° (LZO-like), consistent with a probably formation of crystalline $Ce_2Zr_2O_{7+x}$ or Ce-doped LZO phases with better electrical conduction compared with LZO [16–19]. Third, the secondary phase formation, whatever LZO or LZO-like, tends to reduce in comparison with non added LSM–YSZ at 1350 °C.

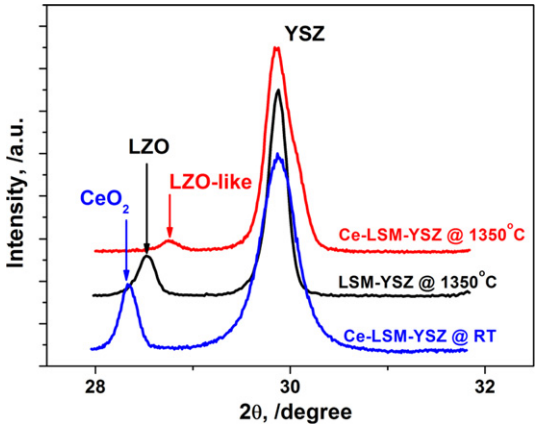

Fig. 4. XRD patterns of Ce–LSM–YSZ at room temperature (RT), LSM–YSZ and Ce–LSM–YSZ pellets sintered at 1350 °C.

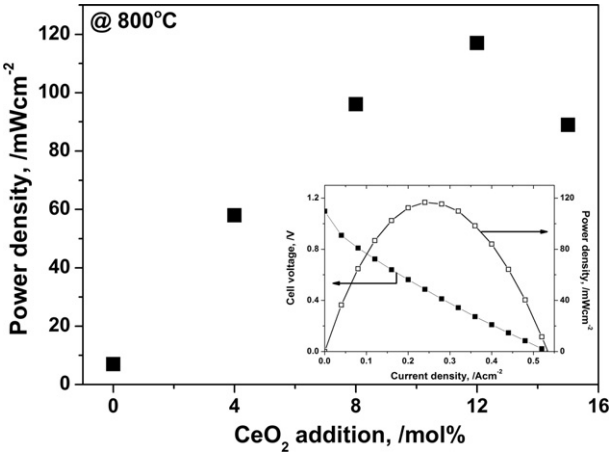

Fig. 5. Power density as a function of CeO_2 addition to $La_{0.8}Sr_{0.2}MnO_3$ at 800 °C. The inset shows the I–V plot for 12 mol% Ce–LSM single cell at 800 °C.

Although XRD and XPS analyses suggest CeO_2 reacts with YSZ at 1350 °C, further experiments will be necessary to characterize the CeO_2 reaction fully and identify any new phase(s) which may have formed at the LSM–YSZ interface. Nevertheless, the results suggest that CeO_2 addition can stabilize the LSM crystal structure and reduce the formation of LZO at high temperature. These are expected to have a beneficial effect on cathode performance after co-sintering with YSZ at high temperature, which we discuss in the next section.

3.2. Cathode and single cell performance after high-temperature sintering

YSZ-electrolyte supported single cells containing Ni–YSZ anode and Ce–LSM cathodes were co-sintered at 1350 °C and then electrochemically evaluated at 800 °C. Fig. 5 shows the power density as a function of CeO_2 addition into LSM. The power density plot shows a significant increase from 7 mW cm^{-2} at $x = 0$ mol% up to a maximum

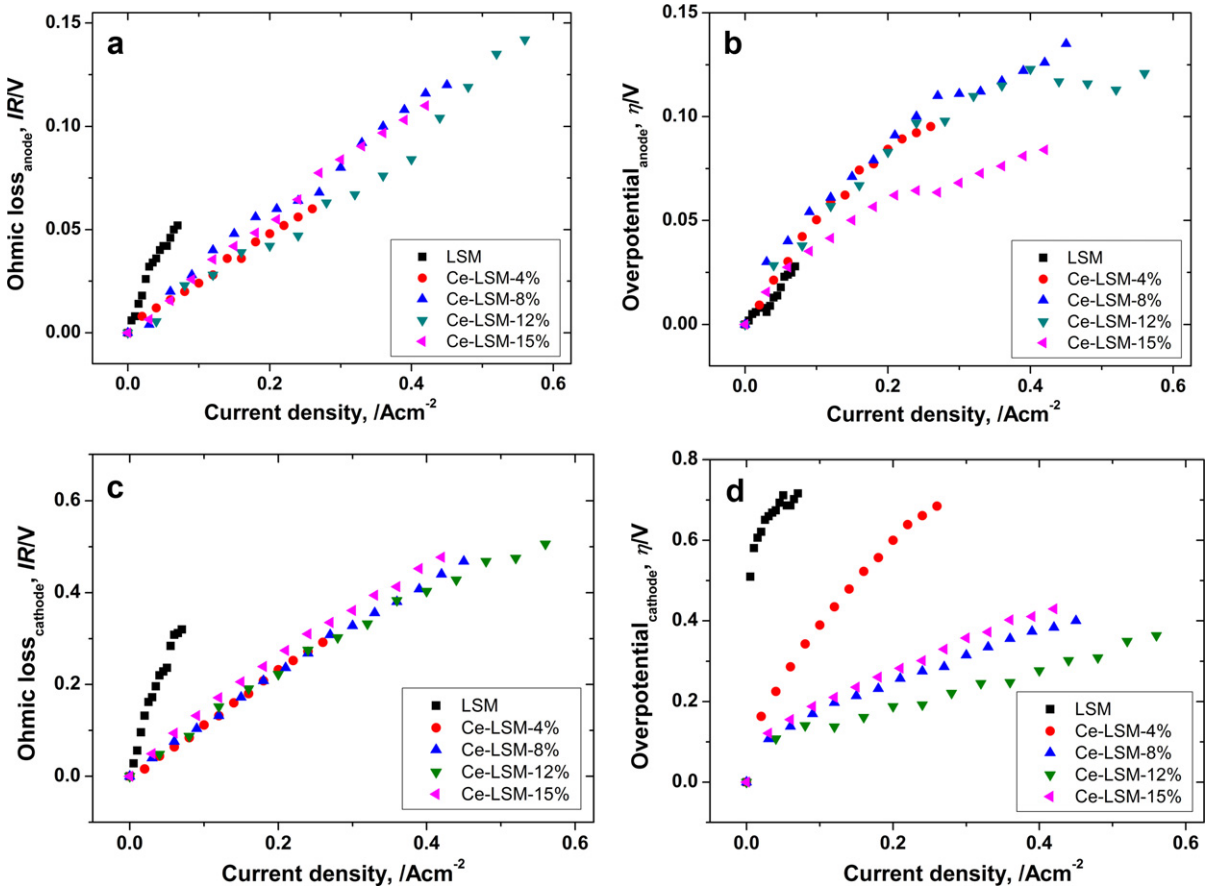

Fig. 6. (a) Ohmic loss and (b) overpotential on the anode side as a function of current density; (c) ohmic loss and (d) overpotential on the cathode side as a function of current density at 800 °C. Suffix indicates the CeO_2 addition in mol%.

of 117 mW cm^{-2} at x = 12 mol%. In other words, a relationship exists between the increase in power density and amount of CeO_2 addition. Furthermore, all samples exhibited 1.1 V of open circuit voltage (OCV) as shown in the inset of Fig. 5, indicating negligible gas leakage and electron conduction through the YSZ electrolyte.

Fig. 6a–d show the ohmic losses (IR) and overpotential (η) at the anode and cathode sides, respectively, for different Ce–LSM cathodes. Fig. 6a and b show that, on the anode side, both ohmic losses and overpotential are almost independent of CeO_2 addition, suggesting no Ce diffusion from cathode to anode. Additionally, both ohmic losses and overpotentials on the anode side are low, indicating the anode is of acceptable quality.

On the other hand, Fig. 6c and d show the ohmic losses and overpotential, respectively, on the cathode side. Fig. 6c shows similar behavior to that in Fig. 6a. However, in Ce–LSM cathodes the ohmic losses are of the same order of magnitude as that observed on the anode side at high current density, whereas ohmic losses of LSM cathodes (without CeO_2 addition) are an order of magnitude higher. Additionally, Fig. 6d shows a clear relationship between overpotential reduction and CeO_2 addition, providing evidence that CeO_2 addition has a large effect on the reduction of overpotential on the cathode side. Furthermore, Ce–LSM cathodes produce overpotential of the same order of magnitude as on the anode side, but for single cells using LSM without CeO_2 as the cathode, in which a large amount of LZO is formed, the overpotential deteriorated drastically. Figs. 5 and 6d thus indicate that the power density enhancement is predominantly a result of the reduction of overpotential on the cathode side.

CeO_2 addition into $La_{0.8}Sr_{0.2}MnO_3$ cathode induces a remarkable increase in power density in YSZ-electrolyte supported single cells sintered at 1350 °C. To the best of our knowledge, this is the highest co-sintering temperature reported for systems exhibiting a reasonable power density without using a buffer layer between the cathode and electrolyte materials, thus simplifying and enhancing the LSM and YSZ co-sintering at high temperature compared with current approaches using buffer layers or similar. Furthermore, because the single cell performance is highly sensitive to the electrolyte thickness, if the electrode thickness is reduced from 300 μm to just a few tens of microns (in an electrode-supported single cell configuration), we expect the power density of single cells sintered at high temperature to exhibit even greater improvement.

4. Conclusions

The thermal stability and electrochemical performance of CeO_2-added LSM cathodes sintered at 1350 °C for 5 h in air were assessed. The results indicate that adding CeO_2 to LSM increases the cathode thermal stability at high temperature. Furthermore, CeO_2 addition to the LSM increases the power density of YSZ-based electrolyte-supported single cells when used as the cathode. The maximum power density obtained in such single cells rose to 117 mW cm^{-2}, compared to a few mW cm^{-2} generated using LSM cathodes without CeO_2. Analysis of the cathode material suggests that cerium could be partially substituted into the LSM crystal lattice, and that CeO_2 addition can modify or reduce the secondary phase formation between the LSM cathode and YSZ electrolyte. Finally, CeO_2 addition seems to be a very simple, convenient and effective strategy for enabling the LSM and YSZ to be co-sintered at 1350 °C during fabrication of SOFC cells. This permits the highest co-sintering temperature reported to date, and results in cells with good power densities without requiring a buffer layer to be introduced between the LSM cathode and YSZ electrolyte.

Acknowledgment

This work has been partially supported by FCO Power Corp.

References

[1] N.Q. Minh, J. Am. Ceram. Soc. 76 (1993) 563.
[2] S.P. Jiang, J. Power Sources 124 (2003) 390.
[3] G.J. Li, Z.R. Sun, H. Zhao, C.H. Chen, R.M. Ren, Ceram. Int. 33 (2007) 1503.
[4] L. Zhang, X. Chen, S.P. Jiang, H.Q. He, Y. Xiang, Solid State Ionics 180 (2009) 1076.
[5] H.Y. Lee, S.M. Oh, Solid State Ionics 90 (1996) 133.
[6] S.P.S. Badwal, Solid State Ionics 143 (2001) 39.
[7] W.-X. Kao, Y.-C. Chang, T.-N. Lin, C.-H. Wang, J.-C. Chang, J. Power Sources 195 (2010) 6468.
[8] M.J. Jørgensen, S. Primdahl, C. Bagger, M. Mogensen, Solid State Ionics 139 (2001) 1.
[9] K. Wiik, C.R. Schmidt, S. Faaland, S. Shamsili, M.-A. Einarsrud, T. Grande, J. Am. Ceram. Soc. 82 (1999) 721.
[10] E. Konysheva, T.S.J. Irvine, A. Besmehn, Solid State Ionics 180 (2009) 778.
[11] V.A.M. Brabers, F.M. van Setten, P.S.A. Knapen, J. Solid State Chem. 49 (1983) 93.
[12] Q.H. Wu, M. Liu, W. Jaegermann, Mater. Lett. 59 (2005) 1480.
[13] M. Marinšek, Mater. Technol. 43 (2009) 79.
[14] JCPDS 73-0444.
[15] E.J. Harvey, K.R. Whittle, G.R. Lumpkin, R.I. Smith, S.A.T. Redfern, J. Solid State Chem. 178 (2005) 800.
[16] F.W. Poulsen, N. Van der Puil, Solid State Ionics 53–56 (1992) 777.
[17] S.N. Achary, S.K. Sali, N.K. Kulkarni, P.S.R. Krishna, A.B. Shinde, A.K. Tyagi, Chem. Mater. 21 (2009) 5848.
[18] T. Sasaki, Y. Ukyo, K. Kuroda, S. Arai, S. Muto, H. Saka, J. Ceram. Soc. Jpn. 112 (2004) 440.
[19] K. Yang, J.-H. Shen, K.-Y. Yang, I.-M. Hung, K.-Z. Fung, M.-C. Wang, J. Power Sources 159 (2006) 63.